

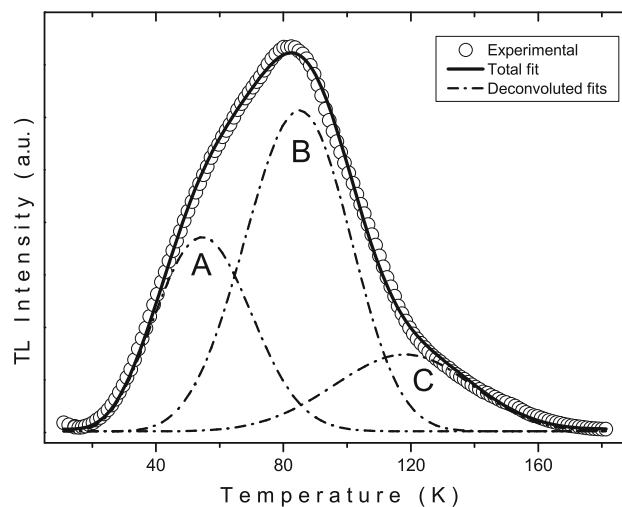
Thermoluminescence properties of ZnO nanoparticles in the temperature range 10–300 K

M. Isik¹ · T. Yildirim² · N. M. Gasanly^{3,4}

Received: 27 April 2015 / Accepted: 16 November 2015 / Published online: 9 December 2015
© Springer Science+Business Media New York 2015

Abstract Low-temperature thermoluminescence (TL) properties of ZnO nanoparticles grown by sol–gel method were investigated in the 10–300 K temperature range. TL glow curve obtained at 0.2 K/s constant heating rate exhibited one broad peak around 83 K. The observed peak was analyzed using curve fitting method to determine the activation energies of trapping center(s) responsible for glow curve. Analyses resulted in the presence of three peaks at 55, 85 and 118 K temperatures with activation energies of 12, 30 and 45 meV, respectively. Thermal cleaning process was applied to separate overlapped peaks and get an opportunity to increase the reliability of results obtained from curve fitting method. Heating rate dependence of glow curve was also studied for rates between 0.2 and 0.7 K/s. The shift of the peak maximum temperatures to higher values and decrease in peak height with heating rate were observed. Moreover, X-ray diffraction and scanning electron microscopy were used for structural characterization.

Graphical Abstract



Keywords Zinc oxide · Nanoparticles · Thermoluminescence · Defects

1 Introduction

Zinc oxide (ZnO) is a promising material for various applications in both microelectronic and optoelectronic devices, especially for optoelectronic light emitting devices in the visible and ultraviolet ranges of the electromagnetic spectrum. ZnO, a member of II–VI group semiconductors, has direct band gap energy of 3.37 eV and large exciton-binding energy of 60 meV [1]. Due to its attractive optical and electrical properties, ZnO has also been an important material used in solar cells, liquid crystal displays,

✉ M. Isik
mehmet.isik@atilim.edu.tr

¹ Department of Electrical and Electronics Engineering, Atilim University, 06836 Ankara, Turkey

² Department of Physics, Nevsehir Haci Bektas Veli University, 50300 Nevsehir, Turkey

³ Department of Physics, Middle East Technical University, 06800 Ankara, Turkey

⁴ Virtual International Scientific Research Center, Baku State University, 1148 Baku, Azerbaijan

semiconducting multilayers, photothermal conversion systems and optical positional sensors [2–6].

The influence of defects on the performance of optoelectronic devices is a well-known subject. In optoelectronic devices such as LEDs or lasers, defects may introduce non-radiative recombination centers which could lower the internal quantum efficiency or, depending on the defect density, even render light generation impossible. In the case of electronic devices, the defects introduce scattering centers lowering carrier mobility, hence hindering high-frequency operation. Therefore, determination of defect center parameters has an important position in both fundamental research and technical applications. One of the methods to determine these parameters is thermoluminescence (TL) which is based on the analysis of temperature dependence of the number of emitted photons existing due to the recombination of excited charge carriers from trap centers with opposite charge carriers in the recombination centers. Previously, TL properties of ZnO materials below and above room temperature have been reported in many papers in the literature. In the above-room-temperature region, TL glow curves of ZnO nanophosphors exhibited two peaks around 420 and 490 K with 0.8 and 1.2 eV activation energies, respectively [7]. TL measurements and analysis on ZnO nanorods showed the presence of two trapping centers at 98 and 190 °C with activation energies of 0.54 and 0.89 eV [8]. In the below-room-temperature region, TL glow curve of ZnO powder exhibited one broad peak in which the presence of five singular peaks at 112, 129, 144, 156 and 172 K was found [9]. Investigations on TL behavior of polycrystalline ZnO resulted with two peaks, a broad peak around 150 K and a well-defined peak at 182 K [10]. Wang et al. [11] investigated the low-temperature thermoluminescence properties of ZnO single crystals obtained from two different companies. Three peaks around 40, 136 and 150 K were observed in the TL glow curves at heating rate of 0.1 K/s. In addition to determination of characteristics of defects, TL method is also used in the area of radiation dosimetry. Previously, dosimetry properties of doped and undoped ZnO were reported in the literature. The dosimetric characteristics of beta irradiated ZnO phosphors synthesized through a controlled chemical reaction were investigated by Borbon-Nunez et al. [12]. The analyses indicated that ZnO phosphors sintered at 1173 K are the most suitable sample for TL dosimetry. TL studies on Mg-doped ZnO nanophosphors showed that Mg doping improves the TL properties of ZnO and carries ZnO to more important position for dosimetry applications [13]. The analyses on TL glow curves of Eu^{3+} and Tb^{3+} -doped ZnO nanorods resulted with 0.9 and 0.8 eV activation energies, respectively. The results also showed that rare-earth-doped ZnO nanorods can be used in TL dosimeter [14].

ZnO materials grown as crystal, thin film and nanostructure can show different properties according to growth method. Recently, ZnO nanostructures have been investigated due to its potential applications in the optoelectronics, photovoltaic and biomedical areas [15, 16]. To the best of our knowledge, low-temperature TL properties of ZnO nanocrystals were not reported in the literature. In the present work, we have performed TL measurements in the temperature range of 10–300 K on ZnO nanocrystals prepared by sol–gel method. Trapping parameters of associated centers were obtained by curve fitting method. Moreover, structural properties of ZnO nanocrystals were investigated by means of X-ray diffraction and scanning electron microscopy experiments.

2 Experimental details

ZnO nanocrystals were prepared by the sol–gel method. A solution of 0.1 M $\text{Zn}(\text{CH}_3\text{COO})_2 \cdot 2\text{H}_2\text{O}$ (zinc acetate dihydrate) was added to a solution of 1 M NaOH (sodium hydroxide) in distilled water using magnetic stirrer while heating at 60 °C. The resulting white solid products were washed with distilled water and ethanol to remove the possible ion remainings in the final products, and it was also calcined at 400 °C for 1 h. Finally, the precursor was pelletized under the pressure of 3 ton before the thermoluminescence measurements. The surface morphology of ZnO nanocrystals was obtained using scanning electron microscope (Nova NanoSEM 430, FEI LTD). X-ray diffraction experiments were performed using Rigaku Miniflex diffractometer with $\text{Cu K}\alpha$ radiation ($\lambda = 0.154049$ nm). The scanning speed of the diffractometer was 0.02°/s.

TL experiments were performed using homemade experimental setup which was built around a closed cycle helium gas cryostat (Advanced Research Systems, Model CSW-202). A Lakeshore Model 331 temperature controller was used to control the sample temperature in the 10–300 K range. A photomultiplier tube, an ultraviolet light source and the relevant optics were connected to the optical access port of the cryostat (quartz window) by a measurement chamber. Luminescence emitted from the crystal was focused by lenses on the photomultiplier tube (Hamamatsu R928; spectral response: 185 to 900 nm) working in photon-counting regime. Pulses from the photomultiplier tube were converted into TTL pulses using a fast amplifier/discriminator (Hamamatsu Photon Counting Unit C3866) and counted by the counter of the data acquisition module (National Instruments, NI-USB 6211). A software program written in LabView™ graphical development environment was used to control whole measurement system/devices. The sample was illuminated

at 10 K for 300 s, experimentally determined time to fill the traps completely. Then, after 120 s of waiting, the sample was heated at constant heating rate and emitted photon counts were recorded as a function of temperature.

3 Results and discussion

Structural properties of ZnO nanoparticles were investigated using X-ray diffraction (XRD) and scanning electron microscopy (SEM) measurements. Figure 1 shows the X-ray diffractogram of as-grown and annealed nanoparticles. The XRD patterns of both samples exhibit peaks at the same positions. However, intensities of the peaks observed for annealed ZnO nanoparticles are higher, and full width at half maximum of peaks is narrower than that of as-grown sample. These are the indications of decrease in the structural disorder and better crystallinity. Miller indices of the diffraction peaks and lattice parameters were obtained from the analysis of diffraction spectra using FullProf.2k computer program. Miller indices (*hkl*) are presented on the diffraction peaks. The lattice parameters of hexagonal unit cell were calculated as $a = 0.3253$ and $c = 0.5214$ nm. These results show good agreement with those of previously reported papers [4]. In order to estimate the size of nanoparticles, Debye–Scherrer's equation was used [17]

$$D = \frac{0.9\lambda}{\beta \cos \theta} \quad (1)$$

where D is crystalline size, β is full width at half maximum, λ is wavelength of X-rays, and θ is diffraction angle. The size of nanoparticles was calculated about 20–45 nm using Eq. 1 for observed diffraction peaks of both as-grown and annealed samples.

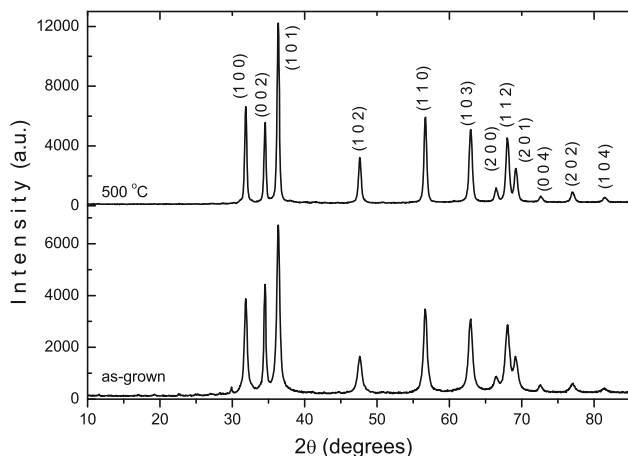


Fig. 1 X-ray powder diffraction of as-grown and annealed ZnO nanoparticles

Surface morphology of the ZnO nanoparticles was characterized using SEM images as shown in Fig. 2. As seen from Fig. 2a, as-grown ZnO nanoparticles aggregate in stacks. When the sample is annealed at 500 °C, the aggregation of nanoparticles decreases evidently and nearly spherical ZnO monodisperse nanoparticles were formed in the samples (see Fig. 2b). The size of the annealed nanoparticles varies in the range of 25–80 nm which is in agreement with calculated size from Scherrer equation.

Thermoluminescence measurements were performed on ZnO nanoparticles in the temperature range of 10–300 K at constant heating rate of $\beta = 0.2$ K/s. Since annealed nanoparticles have better crystalline properties, thermoluminescence properties were investigated on annealed nanoparticles. Figure 3 shows TL glow curve (open circles) in the temperature range in which TL peaks appear. The parameters of trapping center(s) associated with observed peak were found from the analysis of TL glow spectra using curve fitting method. This method is based on fitting of the curve under the light of theoretical expression relating the TL intensity (I_{TL}) to the temperature (T) and activation energy (E_t) of the trapping center as [18]

$$I_{TL} = n_0 v \exp \left\{ -\frac{E_t}{kT} - \int_{T_0}^T \frac{v}{\beta} \exp(-E_t/kT) dT \right\} \quad (2)$$

(for first-order kinetics)

$$I_{TL} = n_0 v \exp \left(-\frac{E_t}{kT} \right) \left[1 + (b-1) \frac{v}{\beta} \int_{T_0}^T \exp(-E_t/kT) dT \right]^{-\frac{b}{b-1}} \quad (3)$$

(for non first-order kinetics)

where n_0 is the initial concentration of trapped charge carriers, v is the attempt-to-escape frequency, T_0 is the starting temperature of heating process, and b is the order of kinetics. The details of this method were reported in our previous work [19]. Fitting process has been performed under the light of Eqs. (2) and (3) for different values of parameter b . The best fitting was accomplished for the presence of three trapping centers and $b = 1.8$, which states the presence of mixed-order kinetics. The experimental (open circles), fitted (solid line) and deconvoluted (dash-dotted) curves corresponding to each center are presented in Fig. 3. The outcomes of curve fitting analysis pointed out the activation energies of trapping centers as 12, 30 and 45 meV with peak maximum temperatures of 55, 85 and 118 K, respectively.

At this point, it will be worthwhile to compare obtained activation energies with previously reported values. The photoluminescence (PL) experiments were performed on

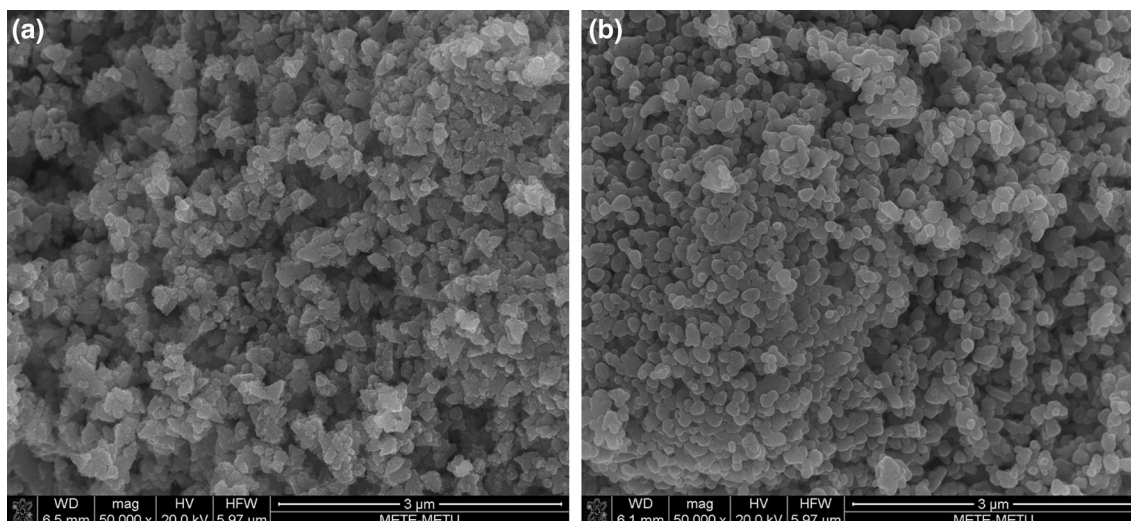


Fig. 2 SEM images of **a** as-grown and **b** annealed ZnO nanoparticles

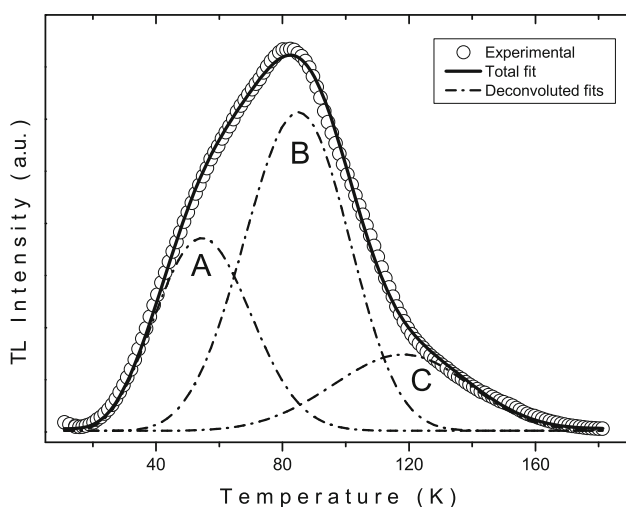


Fig. 3 Experimental TL glow curve (open circles) of ZnO nanoparticles obtained at heating rate of 0.2 K/s. Dash-dotted curves represent the decomposed peaks. Solid curve shows total fit to the experimental data

ZnO quantum dots, Zn nanocrystals and bulk ZnO crystal in the low temperature range of 8.5–300 K [20]. Analysis of the temperature dependence PL intensity resulted with activation energies of 9 and 59 meV for bulk ZnO crystals, 14 meV for ZnO nanocrystals and 9 and 43 meV for ZnO quantum dots. Analysis of temperature-dependent Hall measurements showed the presence of a donor level at 46 meV in ZnO nanocrystals grown by pressure melt growth [21]. Authors attributed the existence of this level to the slightly non-stoichiometric Zn/O ratio which causes the formation of Zn_i representing the dominating donor in the crystal. In another paper focused on temperature-dependent Hall effect measurements on ZnO nanocrystals,

two donor levels at 31 and 61 meV were reported [22]. Look et al. [23] experimentally produced shallow donor at ~ 30 meV by high-energy electron irradiation. Authors identified this donor level as Zn-sublattice defect since production rate is much higher for Zn-face than for O-face irradiation. Taking into account the possible errors, revealed activation energies of 12, 30 and 45 meV in our work are in good agreement with above-given values. However, since our experimental setup and analysis methods do not give opportunity to define the nature of corresponding trapping centers, we avoid giving a specific reason causing these states.

The number of fitting parameters rises with the increase of used deconvoluted peaks. Therefore, the reliability of the results of curve fitting method can be thought as decreasing for more used deconvoluted peaks. We have applied an experimental technique called as thermal cleaning to separate overlapping peaks [18, 24–27]. Thermal cleaning method is applied as follows: The sample illuminated at low temperature ($T_0 = 10$ K) is heated up to a cleaning temperature ($T_{cl} = 40$ K) with rate $\beta = 0.2$ K/s, which is enough to empty the trapping centers giving luminescence at lower temperatures. Then the temperature of the sample is dropped to low temperature (10 K). By this way, trapping center A is emptied, while centers B and C are not affected or lose some of their trapped charge carriers as a negligible amount. When the sample is heated in the whole temperature range (10–180 K) without additional illumination, a new TL glow curve carrying the characteristics of remaining centers B and C is obtained. Figure 4 shows the TL glow curve observed after thermal cleaning procedure. The existence of centers B and C can be clearly seen from this curve. The curve fitting method was also applied to get an opportunity to support the above-

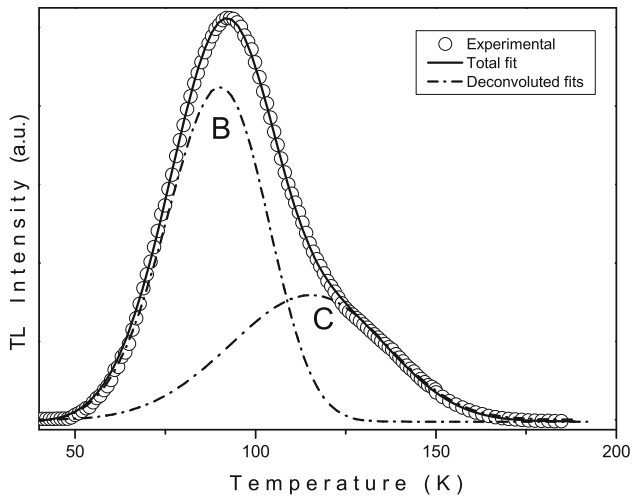


Fig. 4 Experimental TL glow curve (open circles) of ZnO nanoparticles after thermal cleaning for heating rate of 0.2 K/s. Dash-dotted curves represent the decomposed peaks. Solid curve shows total fit to the experimental data

given results before thermal cleaning. The activation energies of centers with peak maximum temperatures of 90 and 116 K were found as $E_{tB} = 35$ meV and $E_{tC} = 45$ meV. The activation energy and peak maximum temperature values corresponding to trapping center C show a good consistency with values obtained before thermal cleaning ($E_{tC} = 45$ meV and $T_{mC} = 118$ K). However, activation energy and peak maximum temperature of center B were found bigger than before thermal cleaning ($E_{tB} = 30$ meV and $T_{mB} = 85$ K). This can be related to existence of distribution of traps. In highly defective materials, trap depths may exhibit a distribution in the forbidden energy gap. When the sample was heated up to a cleaning temperature ($T_{cl} = 40$ K) to empty the trapping center A, some of shallower traps in the distribution of center B were also thought to be emptied. This causes an increase in the activation energy and shift of the peak maximum temperature to higher values ($E_{tB} = 35$ meV and $T_{mB} = 90$ K). Both behaviors supporting the presence of traps distribution were observed for center B after thermal cleaning.

Heating rate dependence of TL curve was also investigated for rates between 0.2 and 0.7 K/s (see Fig. 5). The shift of peak maximum temperature (T_m) to higher values and decrease in peak height were observed as seen from the figure. These behaviors, as suggested by Chen and McKeever [18], are satisfied for observed TL curves. The variation of T_m values with heating rate (β) gives a possibility to determine the activation energies. The dependence of heating rate on T_m is given as [18]

$$\beta = (vk/E_t)T_m^2 \exp(-E_t/kT_m). \quad (4)$$

In this equation, exponential term is the dominant T_m -dependent factor rather than T_m^2 term. Therefore, $\ln(\beta)$

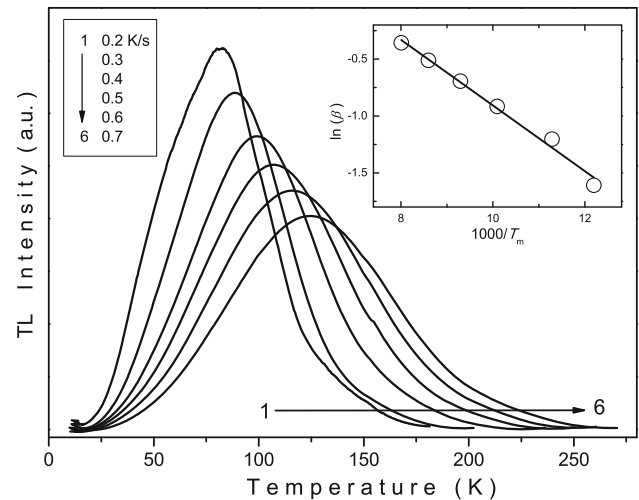


Fig. 5 Experimental TL glow curves of ZnO nanoparticles with different heating rates. Inset: the plot of $\ln(\beta)$ versus $1000/T_m$. Open circles and solid line represent the experimental data and their linear fit, respectively

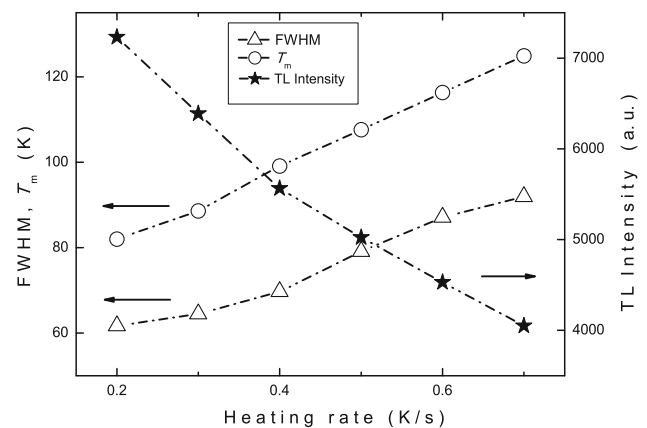


Fig. 6 Dependences of FWHM, peak maximum temperature and TL intensity on heating rates

versus $1/T_m$ plot gives a line with a slope of $-E_t/k$. Inset of Fig. 5 shows this plot (open circles) and its linear fit (solid line). As can be seen from Fig. 3, T_m value of TL glow curve is closer to that of peak B. Therefore, this plot can be strongly associated with peak B. Anyway, the activation energy from the linear fit was found as 28 meV which shows a good agreement with previously obtained value from curve fitting method. Figure 6 indicates the heating rate dependencies of full width at half maximum (FWHM), TL intensity and maximum peak temperature. FWHM of the TL spectra increases with heating rate. Moreover, the increasing and decreasing behaviors of T_m and I_{TL} , respectively, with heating rate obey to TL theory [18].

4 Conclusion

Thermoluminescence measurements were carried out in the low temperature range of 10–300 K on ZnO nanoparticles grown by sol–gel method. TL glow curve observed at heating rate of 0.2 K/s showed one broad peak around 83 K. The analyses of this broad peak revealed the presence of three singular glow peaks at 55, 85 and 118 K. The activation energies of corresponding trapping centers were determined as 12, 30 and 45 meV. Dominant mechanism in the TL process was found as mixed order of kinetics. Heating rate dependency of TL glow curve showed that FWHM and peak maximum temperature increase and TL intensity decreases with heating rate. The activation energy of most intensive peak was found as 28 meV from the analyses of heating rate–peak maximum dependency.

Acknowledgments This work was supported by the Scientific and Technological Research Council of Turkey, 1001 Scientific and Technological Research Projects, No: 110T345.

References

- Kong XY, Wang ZL (2003) *Nano Lett* 3:1625–1631
- Jin BJ, Bae SH, Lee SY, Im S (2000) *Mater Sci Eng B* 71:301–305
- Studeniken SA, Golego N, Cocivera M (1998) *J Appl Phys* 83:2104–2111
- Azam A, Ahmed F, Arshi N, Chaman M, Naqvi AH (2010) *J Alloy Compd* 496:399–402
- Znaidi L (2010) *Mater Sci Eng, B* 174:18–30
- Sahal M, Hartiti B, Ridah A, Mollar M, Mari B (2008) *Microelectronics J* 39:1425–1428
- Pal U, Melendrez R, Chernov V, Barboza-Flores M (2006) *Appl Phys Lett* 89:183118
- Pal PP, Manam J (2013) *Mater Sci Eng, B* 178:400–408
- DeMuer D, Maenhout W (1968) *Physica* 39:123–132
- Seitz MA, Pinter WF, Hirthe WM (1971) *Mater Res Bull* 6:275–282
- Wang Y, Yang B, Can N, Townsend PD (2011) *J Appl Phys* 109:053508
- Borbon-Nunez HA, Cruz-Vazquez C, Bernal R, Kitis G, Furetta C, Castano VM (2014) *Optic Mater* 37:398–403
- Cruz-Vázquez C, Borbón-Nuñez HA, Bernal R, Gaspar-Armenta JA, Castaño VM (2014) *Radiat Eff Defects Solids* 169(5):380–387
- Partha PP, Manam J (2013) *Radiat Phys Chem* 88:7–13
- Wang ZL (2004) *J Phys-Condens Mat* 16:R829–R858
- Ozgur U, Alivov Ya I, Liu C, Teke A, Reshchikov MA, Dogan S, Avrutin V, Cho SJ, Morkoc H (2005) *J Appl Phys* 98:041301
- Cullity BD, Stock SR (2001) *Elements of X-ray diffraction*. Prentice Hall, New Jersey
- Chen R, McKeever SWS (1997) *Theory of thermoluminescence and related phenomena*. World Scientific, Singapore
- Yukseker NS, Gasanly NM, Ozkan H (2003) *Semicond Sci Technol* 18:834–838
- Fonoberov VA, Alim KA, Balandin AA (2006) *Phys Rev B* 73:165317
- Kramer B (ed) (2005) *Adv Solid State Phys* 45:263–274
- Look DC, Reynolds DC, Szelove JR, Lones RL, Litton CW, Cantwell G, Harsch WC (1998) *Sol State Commun* 105:399–401
- Look DC, Hemsley JW (1999) *Phys Rev Lett* 82:2552–2555
- Correcher V, Gomez-Ros JM, Garcia-Guinea J, Lis M, Sanchez-Munoz L (2008) *Radiat Meas* 43:269–272
- Kafadar VE, Yazici AN, Yildirim RG (2009) *J Lumin* 129:710–714
- Macedo ZS, Valerio MEG, de Lima JF (1999) *J Phys Chem Solids* 60:1973–1981
- Kitis G, Furetta C, Prokic M, Prokic V (2000) *J Phys D Appl Phys* 33:1252–1262